Journal of the European Ceramic Society 20 (2000) 1997–2007

Influence of foreign ions on the crystal structure of $BaTiO_3$

M.T. Buscaglia [a], V. Buscaglia [a,*], M. Viviani [a], P. Nanni [b], M. Hanuskova [c]

[a] *Institute of Physical Chemistry of Materials, National Institute of Materials and Related Applications, National Research Council, via De Marini 6, I-16149 Genoa, Italy*
[b] *Department of Chemical and Process Engineering, University of Genoa, Fiera del Mare, Pad. D, I-16129 Genoa, Italy*
[c] *DemoCenter, viale Virgilio 55, I-41100 Modena, Italy*

Received 13 October 1999; received in revised form 18 February 2000; accepted 21 February 2000

Abstract

The influence of dopants (Cr, Co, Fe, Ni, Y, Er, Tb, Gd, Pr and La) on the crystal structure of barium titanate was studied at room temperature and at 250°C using X-ray diffraction. Fine $BaTiO_3$ powders (Ba/Ti = 1.02, size ≈30 nm) have been doped with 1 at% of the foreign element and annealed for 14 and 62 h at two different temperatures: 950 and 1350°C. The room temperature structure of doped $BaTiO_3$ was in any case tetragonal with c/a ratio lower than in the undoped perovskite, but dependent on dopant nature and particle size. For powders calcined at 1350°C, the particle size was in the range 1–5 μm and the decrease in tetragonality was mainly determined by dopant incorporation. Powders treated at 950°C had particles more than one order of magnitude finer (0.1–0.2 μm) and a systematic lowering of the c/a ratio in comparison to the samples annealed at higher temperature was observed. Comparison of the experimental variations of the unit cell edge of cubic $BaTiO_3$ (250°C) with the results of atomistic computer simulations gives indication on the preferential incorporation site of the dopant. In particular, La^{3+} and Pr^{3+} prefer to substitute at the Ba site, whereas Tb^{3+} and Gd^{3+} give partial substitution at the Ti site. For Er^{3+} and Y^{3+} preferential substitution at the Ti site is predicted. For transition metal ions, substitution at the Ti site with oxygen vacancy compensation is confirmed, although their behaviour is less accurately reproduced.

Keywords: $BaTiO_3$; Defects; Doping; Grain size; Impurities

1. Introduction

Doping of $BaTiO_3$-based ceramics is of great importance in the fabrication of electric and electronic devices (multilayer capacitors, heaters and sensors with positive temperature coefficient of resistivity, piezoelectric transducers, ferroelectric thin-film memories, etc.).[1,2] Because of the intrinsic capability of the perovskite structure to host ions of different size, a large number of different dopants can be accommodated in the $BaTiO_3$ lattice. However, the effect of the specific impurity on the electrical conductivity depends on the substitution site (a trivalent ion behaves as an acceptor when substitution occurs at the Ti site or as a donor when it substitutes at the Ba site) as well as on the nature of the defect/electronic charge compensating defect. Addition of donor dopants (Nb^{5+}, La^{3+}) at a relatively low concentration (< 0.5 at%) leads to room-temperature semiconducting ceramics with positive coefficient of resistivity (PTCR) properties, whereas higher dopant contents lead to insulating materials with low concentration of oxygen vacancies and improved resistance to dielectric breakdown. Acceptor-doped $BaTiO_3$ is an insulator at room temperature. Acceptor impurities of the first series of transition metals (Fe, Co, Ni, Cr) are incorporated for the fabrication of multilayer ceramic capacitors to allow for the use of cheaper metal electrodes (i.e. Ni). In fact, the resulting ceramic can be sintered in a reducing atmosphere retaining optimal insulating properties.

The mechanism of dopant incorporation into barium titanate has been largely investigated and a general framework about the behaviour of trivalent impurities in the $BaTiO_3$ lattice can be outlined on the basis of the available literature.[3–17] The ionic radius is the parameter which mainly determines the substitution site. La^{3+} (1.15 Å) and Nd^{3+} (1.08 Å) are exclusively incorporated at the Ba (1.35 Å) site, as their size is incompatible with that of Ti^{4+} (0.68 Å). In fact it has long been known that La^{3+} and Nd^{3+} behave as donors in any case. For the smaller

* Corresponding author.
E-mail address: buscaglia@icfam.ge.cnr.it (V. Buscaglia).

0955-2219/00/$ - see front matter
PII: S0955-2219(00)00076-5

lanthanide ions from Sm^{3+} (1.04 Å) to Lu^{3+} (0.93 Å), it is known that the site occupied by the foreign cation depends on its ionic radius,[15,16] as initially suggested by Rotenberg et al.[6] However, for some ions which were more extensively investigated (Sm^{3+}, Gd^{3+}, Er^{3+} and Y^{3+}) it was found that the substitution site is not exclusive, but is affected by dopant concentration, sintering atmosphere and Ba/Ti molar ratio.[3–5,7,8,15,16] In particular the Ba/Ti ratio seems to play a crucial role. EPR spectra of Gd^{3+} (1.02 Å) in $BaTiO_3$ single crystals[3–5] indicated a preferential substitution on the Ba site, but partial substitution at the Ti site was observed when $Ba/Ti > 1$ and after annealing in reducing atmosphere. Luminescence spectra of Sm^{3+} (1.04 Å) indicated a similar behaviour, with substitution at both the Ba and the Ti site.[6,7] Substitution at the Ti site is enhanced by high dopant concentration. High-temperature electrical conductivity measurements[15] have shown that Er^{3+} (0.96 Å) and Y^{3+} (0.93 Å) behave as acceptors (preferential substitution at Ti site) when $Ba/Ti > 1$ but as donors (preferential substitution at Ba site) when $Ba/Ti < 1$. The electrical conductivity is nearly the same of undoped $BaTiO_3$ when $Ba/Ti = 1$; in such a case the dopant occupies simultaneously both cationic sites, with self-compensation. The dependence of the substitution site of Y^{3+} and Er^{3+} on the Ba/Ti ratio has been confirmed by the room-temperature electrical conductivity measurements and microstructural observations of Xue et al.[16] A recent study of Zhi et al.[17] on $BaTiO_3$ heavily doped with Y^{3+} leads to the same conclusions. For what concerns the ions of the first series of the transition metals, like Cr, Co, Fe and Ni, it is well established and accepted that they preferentially substitute on the Ti site.[9–12] Whilst the rare earth ions examined in the present work (La, Pr, Gd, Tb, Er) and Y exhibit their stable +3 valence state, this is not the case for transition element ions. The valence state of 3d dopants was determined by Ihrig[9] and Hagemann and Ihrig[10] in their extensive work: Cr is incorporated in the +4 state, Fe and Co in the +3 state and Ni in the +2 state when annealing is carried out in air. The corresponding ionic radii (0.55 for Cr^{4+}, 0.64 for Fe^{3+}, 0.63 for Co^{3+} and 0.78 for Ni^{2+}) are compatible with that of Ti^{4+} (0.68). The above ions can be incorporated in the perovskite lattice at least up to 2 at%, a part from Fe^{3+}, which has a solubility of ~1.25 at%.

The effect of dopants on the crystal structure of $BaTiO_3$ has received little attention. Only the effect of the donor dopants Nb^{5+}, La^{3+} and Nd^{3+} was investigated with some detail.[13,14,18–23] The solubility of donor elements in the $BaTiO_3$ lattice is generally high and can exceed 10 at%. There is a general agreement that addition of these ions determines a moderate increase of the *a* lattice parameter and a more pronounced decrease of the *c* lattice parameter resulting in an overall shrinkage of the $BaTiO_3$ unit cell. The structure becomes cubic when the dopant concentration exceeds ≈5 at%. A different behaviour was found for Y^{3+}.[17] When incorporation occurs at the Ba site (up to 1.5 at%) the crystal structure is tetragonal and the unit cell volume increases with the dopant concentration. On the contrary, when incorporation occurs at the Ti site (up to 12 at%), the crystal structure becomes cubic when the Y^{3+} fraction exceeds 6 at%. The unit cell volume increases with the dopant concentration in this case too.

Besides controlling the electrical properties, the presence of dopants considerably affects the microstructure of polycrystalline barium titanate. In particular it is well known that the addition of donor dopants above the critical concentration (0.2–0.5 at%) corresponding to the semiconducting-insulation transition greatly inhibits grain growth.[13,14,16,18,19,21] In heavily-doped ceramics, grain size can be < 1 μm. As a consequence, the influence of grain/particle size on crystal structure of $BaTiO_3$ must be taken into account as a side effect of doping. Pure and large-grained (≈100 μm) polycrystalline $BaTiO_3$ as well as single crystals of macroscopic size have a tetragonal ferroelectric structure at room temperature with lattice constants $c = 4.034$ Å and $a = 3.994$ Å.[24,25] The corresponding c/a ratio is 1.010. The tetragonal modification transforms to the cubic paraelectric phase at 130°C.[2] As the particle size drops below ≈0.5 μm, the c/a ratio rapidly decreases and the cubic modification ($c/a = 1$) becomes stable for particles of 0.1–0.2 μm.[26–32] A similar behaviour was also observed for $PbTiO_3$ and $BaTiO_3$–$PbTiO_3$ solid solutions,[28,33] even though the phase transition occurs at a smaller crystallite size. However, the exact value of particle size for phase transition also depends on $BaTiO_3$ synthesis method and on the agglomeration state of the particles. Powders obtained by the hydrothermal route often possess a cubic or pseudocubic structure. Hennings and Schreinemacher[34] have shown how the protons incorporated in the perovskite lattice during hydrothermal synthesis as OH groups can contribute to stabilize the cubic modification. Transition from the cubic to the tetragonal form in powders with particle size of 0.2–0.3 μm was observed by moderate heating (200–500°C) as a result of water release even though particle size remains constant. Agglomeration is also important: particles that would be cubic if they were isolated, show tetragonal structure when they are part of a cluster.[32] In dense polycrystalline barium titanate, a change from the tetragonal to pseudocubic structure is known to gradually take place at room temperature when grain size < 0.7 μm.[29,35,36] The increase of critical size for phase transition between loose particles and dense ceramics is mainly ascribed to the role of surface effects: solid–gas interfaces have to be considered in the case of powders, whereas solid–solid interfaces become predominant in ceramics.[29] However, the effect of internal stresses in dense, fine grained $BaTiO_3$ ceramics could also affect phase transitions.[35,36]

In the present work we have studied the effect of foreign ions (1 at%) on the crystal structure of $BaTiO_3$ in order to find a correlation between the variation of the unit cell parameters and the prevailing dopant incorporation mechanism. The use of a sub-micron $BaTiO_3$ starting powder (≈30 nm) and two different annealing temperatures has allowed us to obtain a series of "fine" doped powders (0.1–0.2 μm) and a series of "coarse" doped powders (1–5 μm). As a consequence, the effect of crystal size could also be investigated.

2. Experimental

$BaTiO_3$ fine submicron powders were prepared from $Ba(OH)_2$ and $TiCl_4$ using a hydrothermal-like process. The titanium precursor (99.9%, Sigma-Aldrich, Milan, Italy) was slowly introduced in a strong basic $Ba(OH)_2$-NaOH (99%, Aldrich) aqueous solution (pH > 13) kept at 80°C. After 5 h ageing at 80°C, the powder was washed with distilled water until Cl^- ions were completely removed from the supernatant. Both synthesis and washing were carried out under a nitrogen atmosphere to avoid formation of barium carbonate. The details of preparation are described elsewhere.[37] The particle size of the as-prepared powder, as determined by transmission electron microscopy (TEM, model 2010, JEOL, Japan), was in the range of 20–50 nm. The particles consisted of single crystals. The specific surface area, as determined by the BET method (model Gemini 2360, Micromeritics, Norcross, GA, USA), was ≈30 $m^2 g^{-1}$, corresponding to an average particle size of ≈30 nm. The (Ba + Sr)/Ti ratio, as determined by ion-coupled plasma spectroscopy (ICP, model Plasma-2000, Perkin–Elmer, USA) was 1.02. The main impurities present in the powders and determined by ICP analysis were Sr (1.5 at%), Na (85 ppm) and Si (190 ppm). Cl was below 5 ppm. The as-prepared powders were doped with 1 at% of Cr, Co, Fe, Ni, Y, Er, Tb, Gd, Pr and La by wet mixing of 50 g of the titanate powder with an aqueous solution of the corresponding transition metal or rare-earth nitrate (99.9%, Aldrich) in polyethilene jars using zirconia balls. Dopant incorporation was carried out in air by annealing at 950 and 1350°C. Two treatments of different duration were performed: 14 and 62 h. The treatments were conducted in high-purity alumina crucibles (Degussa AL23, 99.7%) using at least 10 g of powder. The particle size of the annealed powders was measured by scanning electron microscopy (SEM, Philips 515, Eindhoven, The Netherlands) on the basis of ≈1000 particles.

The lattice parameters of the $BaTiO_3$ powders at room temperature were determined by powder X-ray diffraction (XRD, model PW1710, Co K_α radiation, secondary graphite monochromator, Philips, Eindhoven, The Netherlands) using the Rietveld method and the DBWS program.[38] For this purpose, the diffraction profile was collected up to the (400) reflection with a step of 0.025 °2θ and a sampling time of 10 s. The lattice parameter of the cubic modification of $BaTiO_3$ was measured at 250°C using a high-temperature X-ray diffractometer (HTXRD, model PW3710, CuK_α radiation, secondary graphite monochromator, heating system Anton Paar ATK, Philips, Eindhoven, The Netherlands) following the same procedure described above, but collecting the diffraction profile up to the (420) reflection. The Rietveld method has given a reasonable fit of the diffraction profiles ($R_{wp} \leqslant 12\%$ for room temperature profiles and $R_{wp} \leqslant 10\%$ for 250°C profiles) except for Y-doped samples annealed for 14 h at 1350°C. In this case an asymmetrical broadening of the diffraction peaks at room temperature as well as at 250°C towards low 2θ angles was noticed. The asymmetry is related to non-homogeneous dopant distribution inside the particles. As a consequence, the lattice parameters obtained for this specific sample have little significance. The asymmetry of the peak profiles disappears when the samples are annealed for 62 h and is absent on samples annealed at 950°C.

3. Results

3.1. Microstructure of doped powders

The particle size of $BaTiO_3$ powders doped with 1 at% of aliovalent impurities and annealed at 950 and 1350°C is reported in Table 1. The size is given as a volume average. The powders treated at 950°C remain in the loose state without appreciable sintering. They are much finer than the powders treated at higher temperature

Table 1
Particle size of thermally treated $BaTiO_3$ pure and doped powders

	Particle size (μm)			
	950°C		1350°C	
Dopant	14 h	62 h	14 h	62 h
Undoped	0.82±0.34		28.0±10.6	
Cr	0.25±0.1	0.66±0.28	5.5±1.9	17.9±3.7
Co	0.11±0.03	0.15±0.06	5.9±2.3	9.2±2.7
Fe[a]	0.16±0.05	0.21±0.09	3.0±1.0	3.8±1.9
				14.8±5.2
Ni	0.09±0.03	0.13±0.04	3.9±1.5	16.0±6.5
Y	0.09±0.02	0.15±0.06	3.3±1.3	6.0±1.9
Er	0.20±0.06	0.20±0.07	4.6±2.2	7.1±2.2
Tb	0.23±0.09	0.31±0.10	3.9±1.2	4.4±1.4
Gd	0.19±0.07	0.19±0.06	2.6±0.9	3.3±1.1
Pr	0.13±0.04	0.16±0.06	0.47±0.17	0.7±0.28
La	0.14±0.05	0.14±0.04	0.41±0.15	0.8±0.28

[a] The particle size distribution of the Fe-doped samples annealed 62 h at 1350°C is bimodal.

with a particle size in the range 0.1–0.2 μm (Fig. 1a); only the particles of undoped barium titanate have grown up to 0.8 μm. The particles generally have a faceted shape, which is distinctly cubic for powders doped with Cr, Fe, Pr and La, as well as for undoped $BaTiO_3$. During annealing at 1350°C further coarsening of the particles occurs (Fig. 1b), with formation of aggregates. Inside the aggregates, partial sintering has occurred, even though the morphology looks dominated by coarsening. In the following, the terms "particle size" and "particle growth" rather than "grain size" and "grain growth" are in any case preferred, even though the distinction is, sometimes, arbitrary. Coarsening is in particular evident in samples doped with transition metal ions, Y and Er, where the average particle size after 62 h annealing is >6 μm. On the contrary, in samples doped with Pr and La particle growth is inhibited and the particle size is only ≈0.7 μm after 62 h. Samples doped with Gd and Tb present an intermediate behaviour: particles have grown up to ≈3–4 μm after 62 h. The Fe-doped powder has a bimodal size distribution, with large particles >10 m and smaller particles of ≈3 μm. Maximum particle growth occurred in the undoped powder, where the particle size exceeds 20 μm.

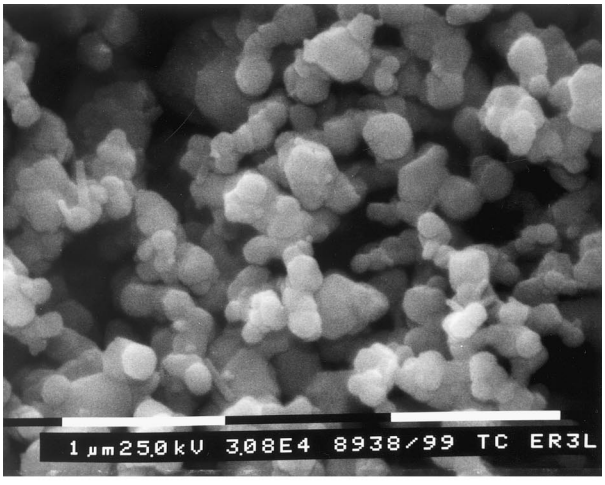

(a)

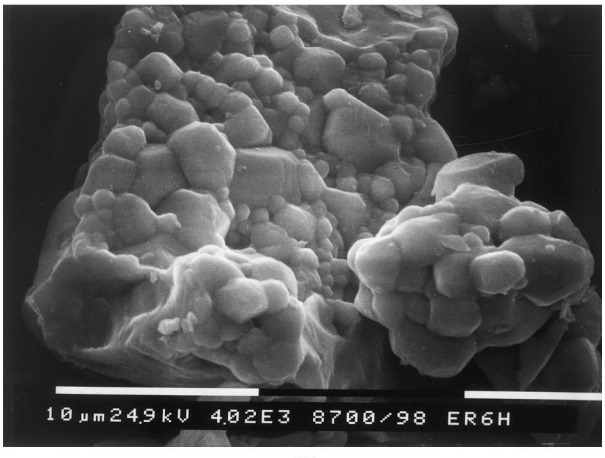

(b)

Fig. 1. SEM micrographs of $BaTiO_3$ powder doped with 1 at% Er; (a) annealed 14 h at 950°C; (b) annealed 14 h at 1350°C.

Powders doped with Cr, Co, Fe and Ni are dark-coloured whereas powders doped with Gd, Pr and La are yellow-coloured. Doping with Tb produces a bright orange colour; powders doped with Y and Er are white. Formation of second phases was not detected in all of the samples within the detection limit of X-ray diffraction (≈0.5 wt%).

3.2. Lattice parameters of tetragonal modification

The room temperature diffractograms were, in any case, fitted with the tetragonal structure. However, in the case of samples doped with Co, Ni and La annealed 14 h at 950°C, and samples doped with Ni annealed 62 h at 950°C, where the tetragonality turns out to be very low ($c/a < 1.003$), the fit with the tetragonal structure is only marginally better than the fit with the cubic structure. The cell parameters of the tetragonal modification as a function of the ionic radius of the dopant are reported in Figs. 2–5. The ionic radius of the transition element ions is that corresponding to the most probable valence state, according to available literature.[9–12] The average error on cell parameters has been estimated to be $\approx \pm 5 \times 10^{-4}$ Å on the basis of repeated collection of diffraction profiles and use of high-purity silicon as internal standard.

The incorporation of dopants leads to an increase of *a* lattice parameter and a decrease of *c* lattice parameter in comparison to undoped $BaTiO_3$. For samples annealed at 950°C (Figs. 2 and 3), the annealing time has a small and poorly significant effect on *a* (except for Fe and Tb), while there is a systematic increase of *c* for all of the

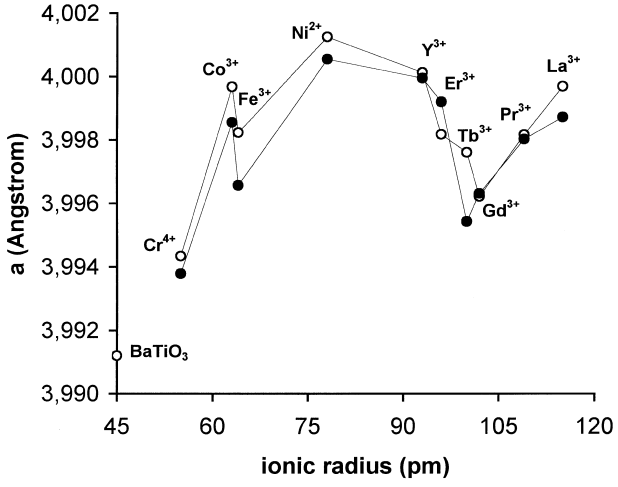

Fig. 2. The lattice parameter *a* of the room temperature tetragonal modification of $BaTiO_3$ as a function of the ionic radius of the dopant for powders annealed at 950°C. (○) Annealing time 14 h. (●) Annealing time 62 h. Dopant fraction: 1 at%. The point corresponding to undoped $BaTiO_3$ (14 h) was placed on the vertical axis as reference.

dopants. For samples annealed at 1350°C (Figs. 4 and 5), there is a noticeable variation of both a and c on increasing the annealing time when doping with Ni and Y. This variation was expected for Y-doped samples, where a non homogeneous dopant distribution in samples annealed for 14 h can be inferred from the observed asymmetric XRD peak profile. Smaller but significant differences are observed also for samples doped with Co, Fe and La. The variation of the reduced lattice parameter of the tetragonal modification, $(a^2c)^{1/3}$, in comparison to undoped $BaTiO_3$, $(a_0^2c_0)^{1/3}$, is shown in Fig. 6 for samples annealed at 950°C and in Fig. 7 for samples annealed at 1350°C. The reduced lattice parameter exhibits a maximum corresponding to either Y^{3+} or Er^{3+}. For samples annealed at 950°C an expansion of the unit cell volume is generally observed (except a very small shrinkage for La- and Pr-doped samples treated for 14 h) and there is a significant volume variation on increasing the annealing time for Y^{3+}, Er^{3+} and Gd^{3+}. For samples annealed at 1350°C, shrinkage of the unit cell is observed for Cr^{4+}, Co^{3+}, Fe^{3+}, Pr^{3+} and La^{3+} incorporation. Unlike the samples annealed at 950°C, the unit cell volume is almost constant with annealing time, with the expected exception of Y. For the remaining ions, the variations are within the experimental error. In the case of Ni, the relative variations of the lattice parameters observed on increasing the annealing time lead to a mutual compensation when the

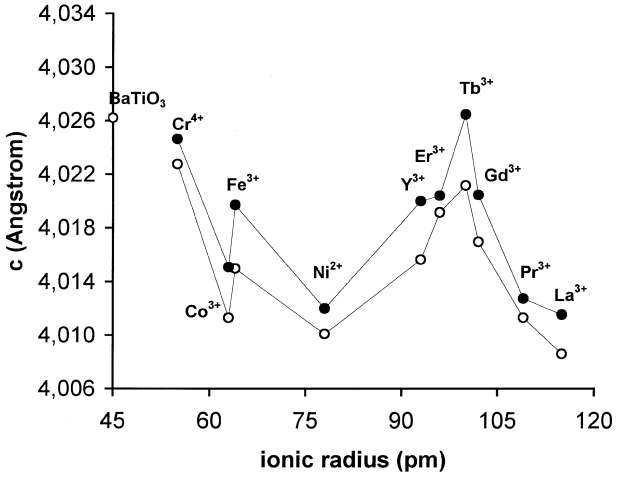

Fig. 3. The lattice parameter c of the room temperature tetragonal modification of $BaTiO_3$ as a function of the ionic radius of the dopant for powders annealed at 950°C. (○) Annealing time 14 h. (●) Annealing time 62 h. Dopant fraction: 1 at%. The point corresponding to undoped $BaTiO_3$ (14 h) was placed on the vertical axis as reference.

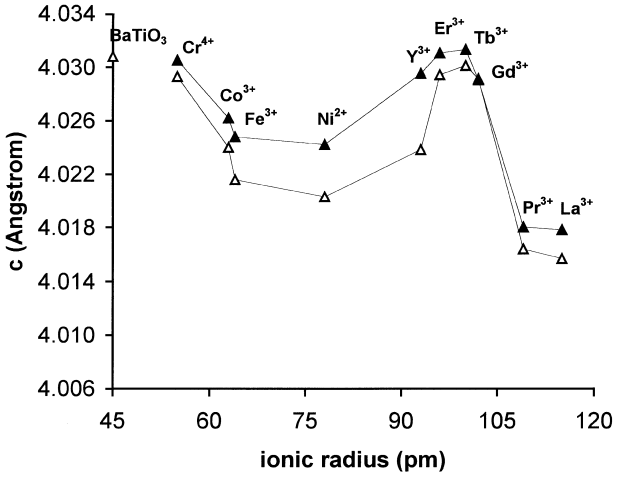

Fig. 5. The lattice parameter c of the room temperature tetragonal modification of $BaTiO_3$ as a function of the ionic radius of the dopant for powders annealed at 1350°C. (△) Annealing time 14 h. (▲) Annealing time 62 h. Dopant fraction: 1 at%. The point corresponding to undoped $BaTiO_3$ (14 h) was placed on the vertical axis as reference.

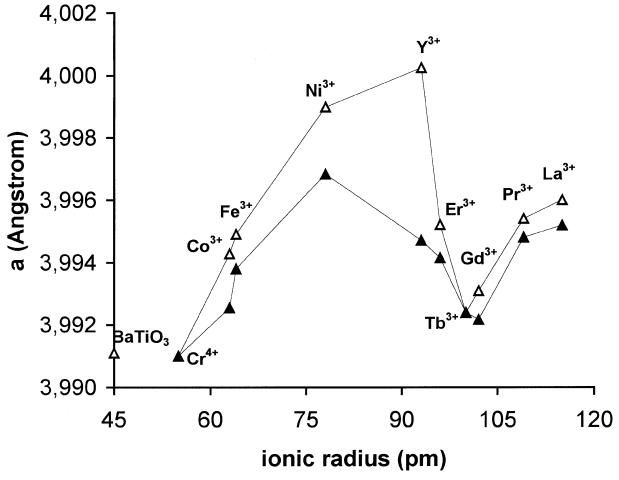

Fig. 4. The lattice parameter a of the room temperature tetragonal modification of $BaTiO_3$ as a function of the ionic radius of the dopant for powders annealed at 1350°C. (△) Annealing time 14 h. (▲) Annealing time 62 h. Dopant fraction: 1 at%. The point corresponding to undoped $BaTiO_3$ (14 h) was placed on the vertical axis as reference.

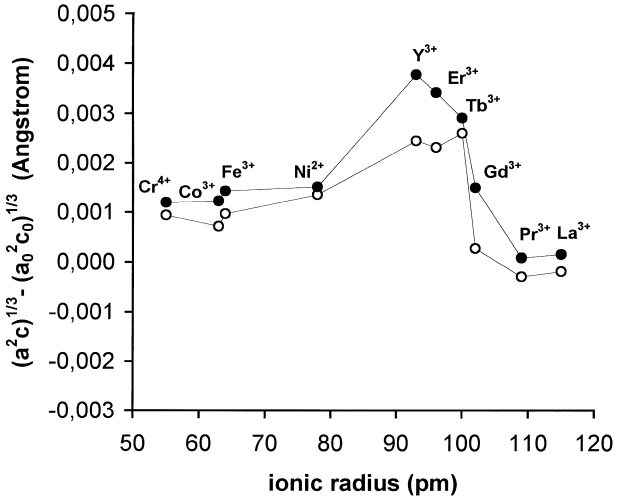

Fig. 6. Variation of the room temperature reduced lattice parameter, $(a^2c)^{1/3}$, of doped (1 at%) $BaTiO_3$ in comparison to that of undoped perovskite, $(a_0^2c_0)^{1/3}$, as a function of the dopant ionic radius for powders annealed at 950°C. (○) Annealing time 14 h. (●) Annealing time 62 h.

unit cell volume is calculated. The c/a ratio as a function of ionic radius of the dopant for the two annealing temperatures (950 and 1350°C) is shown in Fig. 8 for powders fired 14 h and in Fig. 9 for powders fired 62 h. The tetragonality of undoped $BaTiO_3$ annealed at 1350°C perfectly agrees with the literature value reported for single crystals: 1.010.[24,25] The presence of the foreign ion leads to a decrease of the tetragonality of the structure for all of the investigated dopants in comparison to undoped $BaTiO_3$. The decrease of c/a is caused by the increase of a and the decrease of c (see Figs. 2–5). The variation of the c/a ratio with the ionic radius is not monotonic but strongly depends on the nature of the dopant. For samples annealed at 1350°C doping with Cr, Er, Tb and Gd determines only a small variation, whereas for Co, Fe, Ni, Pr and La the decrease in tetragonality is more pronounced. A systematic shift of the points towards lower values of c/a (decreasing tetragonality) can be noticed when the annealing temperature decreases from 1350 to 950°C. The smallest shift is given by undoped $BaTiO_3$ (from 1.010 to 1.0088).

3.3. Lattice parameter of cubic modification

The lattice parameter (a) of the cubic modification measured at 250°C as a function of the ionic radius of the dopant for samples annealed at 1350°C is shown in Fig. 10. The data refer to an annealing time of 14 h,

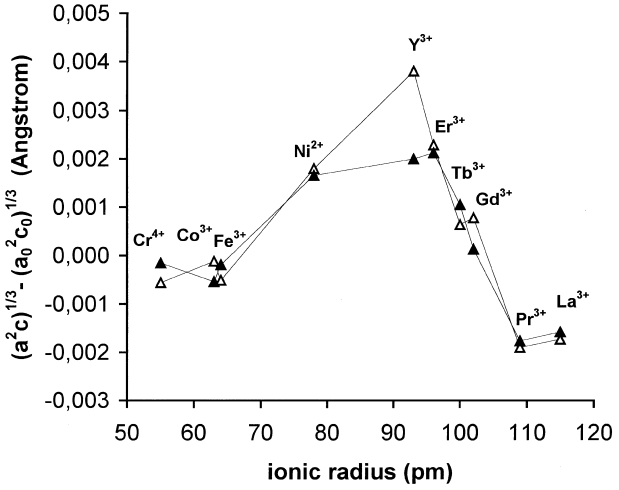

Fig. 7. Variation of the room temperature reduced lattice parameter, $(a^2c)^{1/3}$, of doped (1 at%) $BaTiO_3$ in comparison to that of undoped perovskite, $(a_0^2c_0)^{1/3}$, as a function of the dopant ionic radius for powders annealed at 1350°C. (△) Annealing time 14 h, (▲) annealing time 62 h.

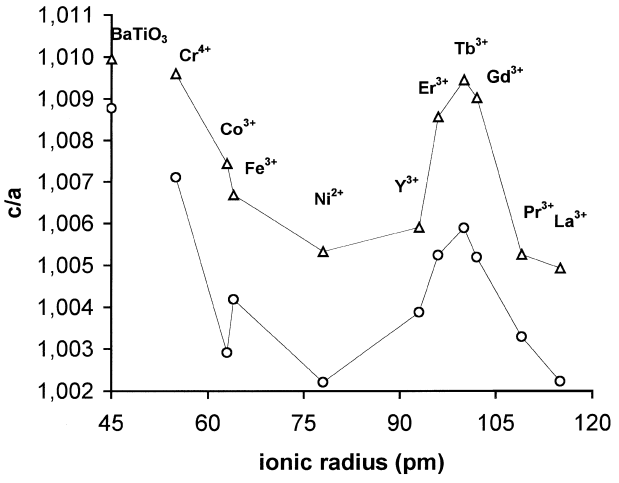

Fig. 8. The room-temperature c/a ratio of doped (1 at%) $BaTiO_3$ as a function of the dopant ionic radius for powders annealed for 14 h. (○) Annealing temperature 950°C, (△) annealing temperature 1350°C. The points corresponding to undoped $BaTiO_3$ (14 h) were placed on the vertical axis as reference.

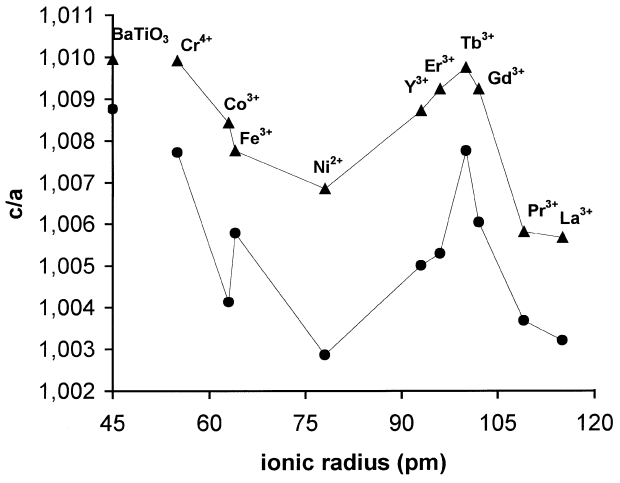

Fig. 9. The room-temperature c/a ratio of doped (1 at%) $BaTiO_3$ as a function of the dopant ionic radius for powders annealed for 62 h. (●) Annealing temperature 950°C, (▲) annealing temperature 1350°C. The points corresponding to undoped $BaTiO_3$ (14 h) were placed on the vertical axis as reference.

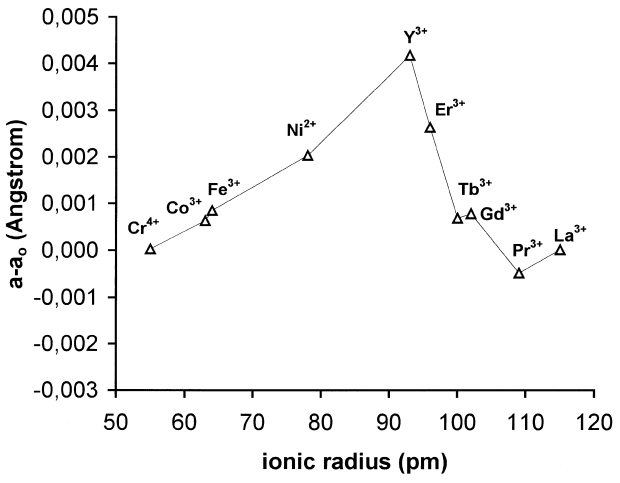

Fig. 10. Variation of the lattice parameter, a, of cubic modification of doped (1 at%) $BaTiO_3$ in comparison to that of undoped perovskite, a_0, as a function of the dopant ionic radius for powders annealed 14 h at 1350°C. For the Y-doped sample, the annealing time was 62 h. Lattice parameter was measured at 250°C.

except for the Y-doped sample, which corresponds to 62 h annealing. The estimated average error on a is of the order of $\pm 5\times10^{-4}$ Å. Comparison of the data of Fig. 10 with the reduced lattice parameter of the tetragonal modification (Figs. 6 and 7) shows, from a qualitative point of view, a similar behaviour: the unit cell volume in both cases passes through a maximum corresponding to either Y^{3+} or Er^{3+}.

4. Discussion

4.1. Dopant diffusion

Dopant incorporation during annealing of the powders occurs by solid-state diffusion. An order of magnitude calculation of the time required to attain homogeneous dopant distribution has been carried out assuming spherical particles of different size. For diffusion in a sphere of radius a, initially ($t = 0$) at uniform concentration $C_1 = 0$, if the surface is maintained at constant concentration C_0, the concentration C at time $t > 0$ and position r ($a > r \geqslant 0$) is given by [39]

$$\frac{C - C_1}{C_0 - C_1} = 1 + \frac{2a}{\pi r}\sum_{n=1}^{\infty}\frac{(-1)^n}{n}\sin\frac{n\pi r}{a}\exp\left(-Dn^2\pi^2 t/a^2\right) \quad (1)$$

where D is the concentration-independent diffusion coefficient. The diffusion in $BaTiO_3$ has been scarcely studied in spite of its fundamental and technological importance related to doping and only limited data are available. Oxygen self-diffusion coefficient ($\approx 2\times10^{-11}$ cm^2 s^{-1} at 1000°C) is much larger than barium self-diffusion coefficient (1.0×10^{-16} cm^2 s^{-1} at 950°C, 8.5×10^{-13} cm^2 s^{-1} at 1350°C).[40] Titanium self-diffusion coefficient is not known. Gopalan and Virkar,[41] in their study on $BaTiO_3$-$SrTiO_3$ interdiffusion at 1300°C, have concluded that Ba is the slowest moving species in the system. For the composition $Ba_{0.4}Sr_{0.6}TiO_3$ they measured an interdiffusion coefficient of $\approx 10^{-11}$ cm^2 s^{-1}. For the same composition, Butler et al.[42] have reported an interdiffusion coefficient of $\approx 2\times10^{-12}$ cm^2 s^{-1} at 1297°C. The authors are not aware of any data about impurity diffusion in $BaTiO_3$. Impurity diffusion in the isostructural $LiNbO_3$ compound is generally of the same order of magnitude of the self-diffusion coefficients [40]. Thus, Eq. (1) has been iteratively solved assuming $C = 0.9C_0$ (the concentration at the centre of the sphere attains 90% of its value at the surface) for different values of the diffusion coefficient and the radius of the particle. It is worth noting that the diffusion time depends quadratically on the radius of the sphere and linearly on the diffusion coefficient. For instance, if $D = 10^{-13}$ cm^2 s^{-1}, uniform dopant incorporation requires 0.021 h for $a = 0.05$ μm, 2.1 h for $a = 0.5$ μm and 210 h for $a = 5$ μm. For $D = 10^{-11}$ cm^2 s^{-1}, the time required for uniform distribution is only 2.1 h for $a = 5$ μm. If $D = 10^{-16}$ cm^2 s^{-1}, the required time increases to 21 h for spheres of radius 0.05 μm. As a consequence, considering the observed size of the $BaTiO_3$ particles (~0.1 μm for powders annealed at 950°C and 3–5 μm for powders annealed at 1350°C) and an annealing time of ≈20 h, a satisfactory uniform dopant distribution can be attained at 950°C if $D \geqslant 10^{-16}$ cm^2 s^{-1} and at 1350°C if $D \geqslant 10^{-12}$ cm^2 s^{-1}. These values compare with the Ba self-diffusion coefficient in $BaTiO_3$. The presence of a large dopant concentration gradient inside the particles of the samples annealed for 14 h should result in an evident change of the lattice parameters on increasing the diffusion time. Large variations of the cell parameters on increasing the annealing time from 14 to 62 h were noticed only for incorporation of Ni^{2+} and Y^{3+} at 1350°C (Figs. 2–5). These variations reflect the existence of a non homogeneous dopant distribution at short annealing times. In particular, the pronounced asymmetry of the XRD peaks of the Y-doped sample can be interpreted as the existence of a core-shell structure within the particles, with two regions of different dopant concentration. On the contrary, the symmetric shape of the XRD peaks of the Ni-doped samples supports the existence of a more uniform concentration gradient. For most part of the remaining samples, the change of the lattice parameter is rather small. This is an indication that a rather homogeneous dopant distribution is already attained after 14 h annealing, although a residual concentration gradient is still present.

4.2. Unit cell volume and incorporation site of dopants

The non-monotonic variation of the unit cell volume as a function of the ionic radius of the dopant ions (Figs. 6, 7 and 10) confirms that the prevailing substitution site is dependent on the ionic radius of the impurity. On the basis of the framework outlined in the Introduction section, the observed behaviour can be interpreted as follows (the notation of Kroger and Vink is used to denote the lattice defects):

(i) The transition element ions (Cr^{4+}, Fe^{3+}, Co^{3+} and Ni^{2+}) preferentially substitute on the Ti site. Incorporation of Cr^{4+} does not require charge compensation,

$$M_2O_3 + 2Ti_{Ti} + \frac{1}{2}O_2 \rightarrow 2M_{Ti} + 2TiO_2 \quad (2)$$

whereas incorporation of Ni^{2+}, Fe^{3+}, Co^{3+} is compensated by the formation of oxygen vacancies, $V_0^{\cdot\cdot}$

$$MO + Ti_{Ti} + O_0 \rightarrow M''_{Ti} + V_0^{\bullet\bullet} + TiO_2 \quad (3)$$

$$M_2O_3 + 2Ti_{Ti} + O_0 \rightarrow 2M'_{Ti} + V_0^{\bullet\bullet} + 2TiO_2 \quad (4)$$

Charge compensation by formation of electron holes can become important only at high oxygen pressure. Expansion of the unit cell occurs when moving from Cr^{4+} (0.55 Å) to Ni^{2+} (0.78 Å) and this is a consequence of the size effect.

(ii) The ions La^{3+} (1.15 Å) and Pr^{3+} (1.09 Å) preferentially substitute at the Ba site

$$2M_2O_3 + 4Ba_{Ba} + Ti_{Ti} \rightarrow 4M^{\bullet}_{Ba} + V'''' _{Ti} + 3BaO + BaTiO_3 \quad (5)$$

The available experimental data[13,14,20] indicate that formation of titanium vacancies, V''''_{Ti}, as charge compensation defects is preferred over formation of barium vacancies when the donor dopant concentration exceeds ≈0.5 at%. Electron compensation prevails only at lower dopant concentration or in reducing conditions. It is worth noting that a small decrease of the unit cell volume occurs in any case when moving from La^{3+} to Pr^{3+}. This is consistent with exclusive substitution at the Ba site (1.35 Å) because of the smaller size of Pr^{3+} in comparison to La^{3+}.

(iii) Moving from Gd^{3+} (1.02 Å) to Y^{3+} (0.93 Å) there is an increasing fraction of the foreign ions substituting at the Ti site. If the trivalent dopant occupies both cationic sites with the same probability, self-compensation occurs

$$M_2O_3 + Ba_{Ba} + Ti_{Ti} \rightarrow M^{\bullet}_{Ba} + M'_{Ti} + BaTiO_3 \quad (6)$$

For Er^{3+} and Y^{3+}, prevalent substitution at the Ti site according to Eq. (4) is likely to occur because of the observed large variation of the unit cell volume. Incorporation at the Ti site is induced by the Ba/Ti molar ratio greater than unity (1.02) in the original powders. If substitution had occurred prevalently at the Ba site a shrinkage would have been observed.

The predicted behaviour of the investigated ions is supported by the results of a recent computer simulation study based on the use of pairwise interatomic potentials within the static lattice approximation.[43] The cell parameter of the cubic modification corresponding to the addition of 1 at% of dopant was computed according to different incorporation mechanisms. Both the foreign ion and the corresponding charge compensating defect (if any) were taken into consideration in the calculation of the unit cell edge. Simulation was carried out on the cubic structure because the tetragonal distorsion of the structure can not be properly described with the adopted pairwise potential. The comparison between the experimentally observed variations of the cell edge induced by the dopant and the calculated variations for (i) substitution at the Ti site with oxygen vacancy compensation [Reactions (3) and (4)], (ii) substitution at the Ba site with titanium vacancy compensation [Reaction (5)] and (iii) substitution at both cationic sites with self-compensation [Reaction (6)] is shown in Fig. 11. The behaviour of the rare earth ions and Y^{3+} is well reproduced. In particular the anticipated incorporation forms corresponding to predominant substitution of La^{3+} and Pr^{3+} at the Ba site, partial substitution of Gd^{3+} and Tb^{3+} at the Ti site and prevalent substitution of Er^{3+} and Y^{3+} at the Ti site are confirmed. The behaviour of the transition impurities is less accurately reproduced. Substitution at the Ti site with oxygen vacancy compensation is the incorporation mechanism which more closely approximates the experimental points. However, a shrinkage of the unit cell is predicted from calculation whereas an expansion is actually observed. One reason for this discrepancy is provided by defect association, which has not been considered in simulation of the dopant effect on lattice parameter.[43] The existence of stable impurity–oxygen vacancy pairs has been reported in $BaTiO_3$ and $SrTiO_3$ doped with iron, cobalt and nickel from EPR measurements.[12] The preferred incorporation mechanism of impurities can also be inferred from the calculation of the solution energy of the dopant oxide[43,44] at infinite dilution. The largest lanthanide ions (La^{3+} and Pr^{3+}) are predicted to substitute at Ba site with electron compensation, whereas for smaller lanthanide ions (Gd^{3+}, Tb^{3+} and Er^{3+}) and Y^{3+}, self-compensation becomes the energetically favoured incorporation mechanism. Even less favoured than electron compensation, titanium vacancy compensation is energetically preferred over barium vacancy compensation. However, the limitations of the static lattice techniques adopted in simulation do not allow to study the effect of thermodynamic variables like the Ba/Ti ratio and the oxygen partial pressure on dopant incorporation. Such parameters can become

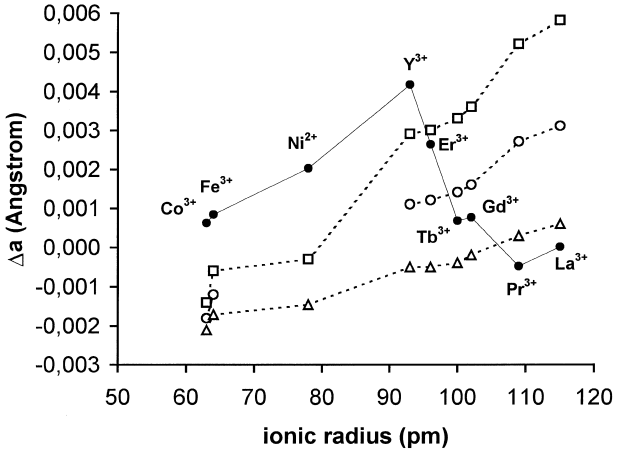

Fig. 11. Calculated (static lattice atomistic simulation) and experimental variation of the lattice parameter of cubic $BaTiO_3$ induced by different dopants (dopant fraction: 1 at%). (□): Incorporation at the Ti site with oxygen vacancy compensation, (○): incorporation by self-compensation, (△): incorporation at the Ba site with titanium vacancy compensation, (●): experimental values (250°C). Substitution of Ni^{2+} at the Ba site does not require charge compensation.

important when the energy difference among different incorporation forms is small. In particular for Y^{3+} and Er^{3+} the energy differences among the mechanisms corresponding to Reactions (4)–(6) are smaller than for any other dopant investigated. This is a further indication of the sensitivity of the substitution site of Er^{3+} and Y^{3+} on Ba/Ti ratio. Calculations also correctly predict the predominant valence state of Fe (+3), Co (+3) and Ni (+2) in the $BaTiO_3$ lattice. For what concerns chromium, our calculations suggest that incorporation in the trivalent state is energetically favoured in contrast with the available experimental data.[9–11] For this reason, the simulation corresponding to Cr^{4+} doping was not included in Fig. 11.

It is worth noting that the addition of aliovalent impurities determines a decrease of the average particle size for all investigated dopants in comparison to pure $BaTiO_3$. For powders treated at 950°C, there are not significative differences between acceptor-doped samples (Fe^{3+}, Co^{3+}, Ni^{2+}, Y^{3+}, Er^{3+}) and the donor-doped samples (La^{3+}, Pr^{3+}) (see Table 1). The particle size changes only of a factor of 2 as a function of the dopant introduced. On the contrary (see Table 1), after firing at 1350°C, the particles of acceptor-doped samples are one order of magnitude larger than those of donor-doped samples (La^{3+}, Pr^{3+}). Also the particle size of Gd- and Tb-doped samples after firing at 1350°C is much larger than that of La- and Pr-doped powders; this observation further supports the hypothesis of partial substitution of these elements on the Ti site.

4.3. Influence of dopants on the c/a ratio

As shown in Figs. 8 and 9, the room-temperature c/a ratio of doped $BaTiO_3$ decreases in comparison to the undoped perovskite for all of the dopants and the nature of the foreign ion has a strong influence on the extent of the effect. Since the particle size of powders annealed at 1350°C is generally of the order of few microns, we can assume that in this case the decrease of tetragonality is mainly induced by dopant incorporation. Only in the case of La and Pr an additional size effect on the room temperature c/a ratio can not be excluded owing to the smaller particle size (≈0.4 μm after 14 h annealing, ≈0.7 μm after 62 h annealing). The ratio of the lattice constants of a $Ba_{0.95}La_{0.01}Sr_{0.04}TiO_3$ single crystal is reported to be ≈1.007.[22] This value can be compared with the ratio found in the present study: 1.005 after 14 h annealing and 1.006 after 62 h annealing. The room temperature c/a ratio measured on dense (99.5%) polycrystalline barium titanate with a grain size of 0.5 μm was ≈1.006.[36] The reduced tetragonality of doped powders annealed at 1350°C can be therefore explained as a stabilization of the cubic phase; as a consequence it is expected to observe a decrease of the Curie temperature, T_c. For doping with Cr, Co, Fe and Ni, the variation of T_c as a function of dopant concentration is reported in Refs. 9 and 10. In any case a decrease of T_c was observed and the value of $-dT_c/dx$, where x is the dopant atomic fraction, rises moving from Cr (≈4°C/1 at%) to Ni (≈30°C/1 at%). In agreement a monotonic decrease of the c/a ratio was found (Figs. 8 and 9). In the case of 1 at% La doping, where the tetragonality is even lower than in Ni doped samples, the T_c is also strongly depressed: 20–40°C/1 at%.[21] The T_c is lowered by ≈10°C/1 at% in Er-doped $BaTiO_3$[6] and by 29°C/1 at% in ceramics of composition $BaTi_{1-x}Y_xO_3$ (Ti site substitution).[45] Concerning the remaining dopants (Tb, Gd) the authors are not aware of literature data about their effect on T_c.

The stabilization of the cubic phase in the case of Co^{3+}, Fe^{3+} and Ni^{2+} is the consequence of two effects:[9,10,12] (i) the creation of oxygen vacancies as charge compensating defects (ii) the symmetry properties of the electronic wave functions of the unfilled 3d shell of the above transition metal ions, which impede bonding with the p oxygen orbitals. The most thoroughly investigated dopant in this category is Fe^{3+}.[12] It was found that Fe^{3+} participates by less than one order of magnitude to the collective offcentre displacement of Ti^{4+} ions during the cubic to tetragonal transition in $BaTiO_3$. In other words it remains at the approximate centre of the oxygen octahedron, opposing to phase transition.

4.4. Influence of particle size on the c/a ratio

The lowering of the annealing temperature from 1350 to 950°C has a considerable influence on the room-temperature c/a ratio of doped $BaTiO_3$ (Figs. 8 and 9). The observed, sistematic reduction of tetragonality is a direct consequence of the smaller size (0.1–0.2 μm) of the particles obtained at 950°C in comparison to annealing at higher temperature (1–5 μm). The observed c/a ratio in powders treated at 950°C thus corresponds to the superposition of the intrinsic effect of doping on crystal structure and of the particle size effect, which is a side-effect of dopant addition. The size of doped powders annealed at 950°C falls in the critical range where a strong reduction of the room-temperature c/a ratio is observed for pure $BaTiO_3$.[26–32] For undoped $BaTiO_3$, where the smallest decrease in tetragonality is observed (from 1.010 to 1.009), the particles obtained at 950°C are substantially larger (≈0.8 m) than those of doped powders (0.1–0.2 μm). A size effect on the $BaTiO_3$ crystal structure similar to that described in the present work and induced by La doping was reported by Hsiang et al.[46] Fine perovskite powders containing 2 at% La showed cubic structure after firing at 900 and 1000°C, but tetragonal structure after annealing at 1100 and 1200°C. The undoped crystallites had tetragonal structure irrespective of temperature. The different behaviour

was attributed to the inhibition of particle growth induced by doping.

Examination of Figs. 8 and 9 reveals that the c/a ratio increases when the annealing time passes from 14 to 62 h. For samples treated at 1350°C, the main reason for this behaviour is a more uniform dopant distribution attained after a longer annealing time. Accordingly, the observed variation is larger for Ni- and Y-doped samples. In the case of powders treated at 950°C, also the particle size effect is likely to have an important role in the increase of tetragonality. Although the average particle size only increases of ≈30%, a variation of this extent can have a non-negligible effect on the tetragonality of the structure for particles in the range 0.1–0.2 μm as verified for undoped $BaTiO_3$.[26–32]

5. Conclusions

Fine $BaTiO_3$ powders (Ba/Ti = 1.02, size ≈30 nm) were doped with 1 at% of different dopants: Cr, Co, Fe, Ni, Y, Er, Tb, Gd, Pr and La. Dopant incorporation has been carried out by annealing at 950 and 1350°C in air. The lattice parameters at room-temperature as well as at 250°C were measured by X-ray diffraction using the Rietveld method. The following conclusions can be drawn from the present study:

1. The room-temperature structure of doped $BaTiO_3$ is tetragonal.
2. The room-temperature c/a ratio of doped $BaTiO_3$ is lower than that of undoped $BaTiO_3$ (1.01) for all the investigated dopants, but dependent on the dopant nature and annealing temperature. For powders doped with Co, Ni and La and annealed at 950°C, the tetragonality is < 1.003.
3. The c/a ratio of doped $BaTiO_3$ powders annealed at 1350°C is mainly determined by dopant incorporation.
4. The c/a ratio of doped $BaTiO_3$ powders annealed at 950°C results from the combined effect of dopant incorporation and particle size. In this case the particle size (0.1–0.2 μm) was more than one order of magnitude smaller than in powders calcined at 1350°C.
5. Comparison of the experimentally measured unit cell edge of cubic $BaTiO_3$ (250°C) with the results of atomistic computer simulations gives indication on the preferential incorporation site of the dopants. In particular, La^{3+} and Pr^{3+} prefer to substitute at the Ba site whereas Tb^{3+} and Gd^{3+} give partial substitution at the Ti site. For Er^{3+} and Y^{3+} preferential substitution at the Ti site is predicted in the present case. For transition metals impurities, preferential substitution at the Ti site is confirmed, although the observed behaviour is less accurately reproduced by simulations.

Acknowledgements

The authors wish to thank Mr. C. Bottino for SEM investigation and Mr. A. Testino for ICP analysis.

References

1. Moulson, A. J. and Herbert, J. M., *Electroceramics*. Chapman & Hall, London, 1990.
2. Jaffe, B., *Piezoelectric Ceramics*. Academic Press, London, 1971.
3. Rimai, L. and deMars, G. A., Electron paramagnetic resonance of trivalent gadolinium ions in strontium and barium titanates. *Phys. Rev.*, 1962, **127**, 702–710.
4. Takeda, T. and Watanabe, A., Two sets of ESR of Gd^{3+} in $BaTiO_3$ ceramic semiconductor. *J. Phys. Soc. Jap.*, 1964, **19**, 1742.
5. Takeda, T. and Watanabe, A., Electron spin resonance of Gd^{3+} in reduced $BaTiO_3$. *J. Phys. Soc. Japan*, 1966, **21**, 1132–1136.
6. Rotenberg, B. A., Danilyuk, Yu.L., Gindin, E. I. and Prokhvatilov, V. G., Electrical and radiospectroscopic investigations of barium titanate with admixtures of oxides of trivalent elements. *J. Sov. Phys.-Solid State*, 1966, **7**, 2465–2469.
7. Murakami, T., Nakahara, M., Miyashita, T. and Ueda, S., Electrical conduction of rare-earth-doped $BaTiO_3$ single crystals. *J. Am. Ceram. Soc.*, 1973, **56**, 291–293.
8. Murakami, T., Miyashita, T., Nakahara, M. and Sekine, E., Effect of rare-earth ions on electrical conductivity of $BaTiO_3$ ceramics. *J. Am. Ceram. Soc.*, 1973, **56**, 294–297.
9. Ihirg, H., The phase stability of $BaTiO_3$ as a function of doped 3d elements: an experimental study. *J. Phys. C. Solid State Phys.*, 1978, **11**, 819–827.
10. Hagemann, H.-J. and Ihrig, H., Valence change and phase stability of 3d-doped $BaTiO_3$ annealed in oxygen and hydrogen. *Phys. Rev. B.*, 1979, **20**, 3871–3878.
11. Hagemann, H.-J. and Hennings, D., Reversible weight change of acceptor-doped $BaTiO_3$. *J. Am. Ceram. Soc.*, 1981, **64**, 590–594.
12. Muller, K. A., Paramagnetic point and pair defects in oxide perovskites. *J. Physique*, 1981, **42**, 551–557.
13. Chan, H. M., Harmer, M. P. and Smyth, D. M., Compensating defects in highly donor-doped $BaTiO_3$. *J. Am. Ceram. Soc.*, 1986, **69**, 507–510.
14. Shaikh, A. S. and Vest, R. W., Defect structure and dielectric properties of Nd_2O_3-modified $BaTiO_3$. *J. Am. Ceram. Soc.*, 1986, **69**, 689–694.
15. Takada, K., Chang, E. and Smyth, D. M., Rare earth additions to $BaTiO_3$. *Advan. Ceram.*, 1987, **19**, 147–152.
16. Xue, L. A., Chen, Y. and Brook, R. J., The influence of ionic radii on the incorporation of trivalent dopants into $BaTiO_3$. *Mater. Sci. Eng.*, 1988, **B1**, 193–201.
17. Zhi, J., Chen, A., Zhi, Y., Vilarinho, P. M. and Baptista, J. L., Incorporation of yttrium in barium titanate ceramics. *J. Am. Ceram. Soc.*, 1999, **82**, 1345–1348.
18. Belous, A. G., V'yunov, O. I. and Khomenko, B. S., Microstructure and semiconducting properties of barium titanate containing heterovalent substituents on the titanium site. *Inorganic Materials*, 1998, **34**, 597–601.
19. Buessem, W. R. and Kahn, M., Effects of grain growth on the distribution of Nb in $BaTiO_3$ ceramics. *J. Am. Ceram. Soc.*, 1971, **54**, 458–461.

20. Jonker, G. H. and Havinga, E. E., The influence of foreign ions on the crystal lattice of barium titanate. *Mater. Res. Bull.*, 1982, **17**, 345–350.
21. Kurata, N. and Kuwabara, M., Semiconducting-insulating transition for highly donor-doped barium titanate ceramics. *J. Am. Ceram. Soc.*, 1993, **76**, 1605–1608.
22. Motohira, N., Okamoto, H., Nakamura, Y., Kishimoto, A., Miyayama, M. and Yanagida, H., Single crystal growth and electrical properties of lanthanum- and gadolinium-doped $BaTiO_3$. *J. Ceram. Soc. Japan*, 1996, **104**, 264–267.
23. Kutty, T. R. N. and Murugaraj, P., Phase relations and dielectric properties of $BaTiO_3$ ceramics heavily substituted with neodymium. *J. Mater. Sci.*, 1987, **22**, 3652–3664.
24. Kay, H. F., Vellard, H. J. and Vousden, P., *Nature*, 1949, **163**, 636–637.
25. Harada, J., Pedersen, T. and Barnea, Z., X-ray and neutron diffraction study of tetragonal barium titanate. *Acta Cryst.*, 1970, **B26**, 336–344.
26. Uchino, K., Sadanaga, E. and Hirose, T., Dependence of the crystal structure on particle size in barium titanate. *J. Am. Ceram. Soc.*, 1989, **72**, 1555–1558.
27. Yen, F.-S., Chang, C. T. and Chang, Y.-H., Characterization of barium titanyl oxalate tetrahydrate. *J. Am. Ceram. Soc.*, 1990, **73**, 3422–3427.
28. Saegusa, K., Rhine, W. E. and Bowen, H. K., Effect of composition and size of crystallite on crystal phase in lead barium titanate. *J. Am. Ceram. Soc.*, 1993, **76**, 1505–1512.
29. Caboche, G. and Niepce, J. C., Dielectric constant of fine grain $BaTiO_3$. *Ceram. Trans.*, 1993, **32**, 339–345.
30. Kataoka, M., Suda, K., Ishizawa, N., Marumo, F., Shimizugawa, Y. and Ohsumi, K., Determination of the c/a ratio of a submicrometer-sized crystal of tetragonal barium titanate by the synchrotron radiation. *J. Ceram. Soc. Japan*, 1994, **102**, 213–216.
31. Begg, B. D., Vance, E. R. and Nowotny, J., Effect of particle size on the room-temperature crystal structure of barium titanate. *J. Am. Ceram. Soc.*, 1994, **77**, 3186–3192.
32. Li, X. and Shih, W.-H., Size effects in barium titanate particles and clusters. *J. Am. Ceram. Soc.*, 1997, **80**, 2844–2852.
33. Ishikawa, K., Yoshikawa, K. and Okada, N., Size effect on the ferroelectric phase transition in $PbTiO_3$ ultrafine particles. *Phys. Rev. B: Condens. Matter.*, 1988, **37**, 5852–5855.
34. Hennings, D. and Schreinemacher, S., Characterization of hydrothermal barium titanate. *J. Eur. Ceram. Soc.*, 1992, **9**, 41–46.
35. Artl, G., Hennings, D. and de With, G., Dielectric properties of fine-grained barium titanate ceramics. *J. Appl. Phys.*, 1985, **58**, 1619–1625.
36. Bell, A. J. and Moulson, A. J., The effect of grain size on the dielectric properties of barium titanate ceramic. *Br. Ceram. Proc.*, 1985, **36**, 57–66.
37. Leoni, M., Viviani, M., Nanni, P. and Buscaglia, V., Low-temperature aqueous synthesis (LTAS) of ceramic powders with perovskite structure. *J. Mater. Sci. Lett.*, 1996, **15**, 1302–1304.
38. Wiles, D. B. and Young, R. A., A new computer program for Rietveld analysis of X-ray powder diffraction patterns. *J. Appl. Cryst.*, 1981, **14**, 149–151.
39. Crank, J., *The mathematics of diffusion*. Oxford University Press, London.
40. Freer, R., Bibliography self-diffusion and impurity diffusion in oxides. *J. Mater. Sci.*, 1980, **15**, 803–824.
41. Gopalan, S. and Virkar, A. V., Interdiffusion and Kirkendall effect in doped barium titanate-strontium titanate diffusion couples. *J. Am. Ceram. Soc.*, 1995, **78**, 993–998.
42. Butler, E. P., Jain, H. and Smyth, D. M., Interdiffusion of alkaline earth cations in their titanates. *Defect Diffusion Forum*, 1989, **66-69**, 1519–1524.
43. Buscaglia, M. T., Buscaglia, V., Viviani, M. and Nanni, P., Atomistic simulation of dopant incorporation in $BaTiO_3$, submitted to *J. Am. Ceram. Soc.*
44. Lewis, G. V. and Catlow, C. R. A., Simulation studies of doped and undoped barium titanate using computer simulation techniques. *J. Phys. Chem. Solids*, 1986, **47**, 89–97.
45. Zhi, J., Chen, A., Zhi, Y., Vilarinho, P. M. and Baptista, J. L., Dielectric properties of $Ba(Ti_{1-y}Y_y)O_3$ ceramics. *J. Appl. Physics*, 1998, **84**, 983–986.
46. Hsiang, H.-I., Yen, F.-S. and Chang, Y.-H., Effects of doping with La and Mn on the crystallite growth and phase transition of $BaTiO_3$ powders. *J. Mater. Sci.*, 1996, **31**, 2417–2424.